Plant Cell Tiss Organ Cult (2013) 113:257–267
DOI 10.1007/s11240-012-0265-z

ORIGINAL PAPER

Cloning and characterization of phenylalanine ammonia-lyase in medicinal *Epimedium* species

Shaohua Zeng · Yilan Liu · Caiyun Zou · Wenjun Huang · Ying Wang

Received: 23 August 2012 / Accepted: 20 November 2012 / Published online: 27 November 2012

Abstract Phenylalanine ammonia-lyase (PAL) plays an important role in the phenylpropanoid pathway and in accumulation of major secondary metabolites in medicinal *Epimedium* species, including icariin, epimedin A, epimedin B, and epimedin C (hereafter designated as active components). In this study, three *Epimedium sagittatum PALs* (*EsPALs*) mRNA sequences, designated respectively as *EsPAL1*, *EsPAL2* and *EsPAL3* deduced to encode 708, 716, and 739 amino acids, were isolated and characterized. Based on sequence and phylogenetic analyses, *EsPAL1* was found to be closer to *EsPAL2* than to *EsPAL3*. Spatio-temporal expression profiles and metabolic accumulation profiles revealed that *EsPAL3* was highly expressed in flavonoid-enriched tissues and leaves at certain developmental stages along with high levels of active components, while *EsPAL1* was highly expressed in leathery leaves along with high lignin content. Under light stress, the total flavonoid content was enhanced by 100 μM phytohormones tested or 5 % sucrose through upregulating different *EsPAL* isoform(s). Our findings have laid a solid foundation for improving the content of bioactive components in *Epimedium* via metabolically engineering *EsPAL*.

Keywords PAL · *Epimedium* · Bioactive components · Phytohormone · Light stress

Abbreviations

RACE	Rapid amplification of cDNA ends
ORF	Open reading frame
PAL	Phenylalanine ammonia-lyase
EsPAL	*Epimedium sagittatum* PAL
ABA	Abscisic acid
GA_3	Gibberellic acid
Suc	Sucrose
IAA	Indole-3-acetic acid
SA	Salicylic acid
RT	Room temperature
MIO	3,5-dihydro-5-methylidene-4H-imidazol-4-one

Introduction

Epimedium L. is known as Barrenwort and Yin Yang Huo in Chinese, and it is also nicknamed "three branches–nine leaves grass" for having three petioles on its rhizome and three leaves on each petiole. Five *Epimedium* species, namely *E. sagittatum* Maxim, *E. brevicornu* Maxim,

Electronic supplementary material The online version of this article (doi:10.1007/s11240-012-0265-z) contains supplementary material, which is available to authorized users.

S. Zeng · C. Zou
Key Laboratory of Plant Resources Conservation and Sustainable Utilization, South China Botanical Garden, Chinese Academy of Sciences, Guangzhou 510650, People's Republic of China
e-mail: shhzeng@scbg.ac.cn

C. Zou
e-mail: zoucaiyun-19851010@163.com

Y. Liu · W. Huang · Y. Wang (✉)
Key Laboratory of Pant Germplasm Enhancement and Speciality Agriculture, Wuhan Botanical Garden, Chinese Academy of Sciences, Wuhan 430074, Hubei, People's Republic of China
e-mail: oryzalin2000@yahoo.com.cn

Y. Liu
e-mail: liuyilan11@163.com

W. Huang
e-mail: hzauhwj@gmail.com

E. pubescens Maxim, *E. wushanense* T. S. Ying, and *E. koreanum* Nakai, are registered in the Pharmacopoeia of the People's Republic of China (Committee 2005) due to their high contents of active compounds. So far, more than 260 compounds have been identified in the genus *Epimedium* with prenyl-flavonol derivatives being the major active components used as chemotaxonomic markers (Ma et al. 2011c). Especially, epimedin A, epimedin B, epimedin C, and icariin (hereafter designated as active components) are defined by the China Pharmacopoeia Committee as major standards for evaluating *Epimedium* quality (Committee 2005). Several lines of studies have reported that *Epimedium* flavonoid compounds can strengthen kidney, cure rheumatism and osteoporosis, benefit coronary heart patients, improve immunity, postpone caducity, and reduce tumor propagation (Ma et al. 2011c; Zhu et al. 2011; Tong et al. 2011). However, most previous studies have been focused on extracting and identifying novel phenolic metabolites. While an *E. sagittatum* 454 EST database has been established (Zeng et al. 2010), the molecular mechanism of the phenylpropanoid biosynthesis pathway in *Epimedium* L. still remains unclear (Fig. 1).

The phenylpropanoid pathway plays a pivotal role in the modulation of several secondary metabolites (caffeic acids, flavonoids, isoflavonoids, lignins, coumarins, salicylic acids (SAs), phytoalexins, chlorogenic acids, and stilbenes) responsible for biological functions such as plant development regulation, disease resistance, signal transduction, and pollination attraction. Phenylalanine ammonia-lyase (PAL; EC 4.3.1.5), a rate-limiting enzyme in the phenylpropanoid pathway, concatenates primary and secondary metabolites by carrying out the first catalysis step in the biosynthesis of the phenylpropanoid pathway via

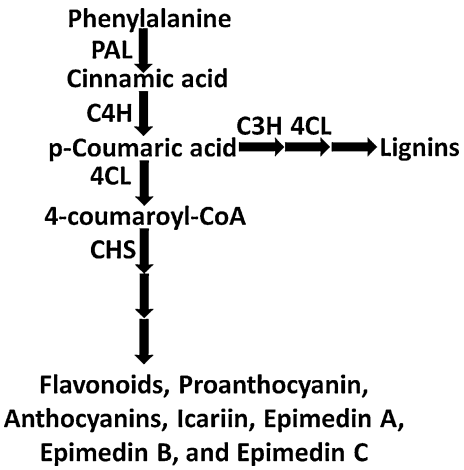

Fig. 1 A simplified schematic pathway for phenylpropanoid biosynthesis in *Epimedium*. Enzyme abbreviations: *PAL* phenylalanine ammonia-lyase, *CHS* chalcone synthase, *C4H* cinnamate 4-hydroxylase, *4CL* 4-coumaroyl: CoA-ligase, *C3H* p-coumarate 3-hydroxylase

catalyzing the non-oxidative deamination of L-phenylalanine to form trans-cinnamic acid and ammonia. Several *PAL* genes have been isolated from several plants, including *Salvia miltiorrhiza* (Song and Wang 2009), *Angelica gigas* (Park et al. 2010), and *Solanum lycopersicum* (Guo and Wang 2009). In short, *PAL* exists in plants with a small multiple-gene family (Guo and Wang 2009; Huang et al. 2010; Reichert et al. 2009).

Flavonoid biosynthesis is differentially modulated by different external (environmental) and internal (developmental) factors, such as the quality of light and stresses like wound (Xu et al. 2008), low temperature (Guo and Wang 2009), infection, nutrition, and phytohormones (Guo and Wang 2009; Jiang and Joyce 2003). Furthermore, flavonoids are synthesized in specific cells and/or organs at particular developmental stages and induced by certain stimuli. So far, to the best of our knowledge, no reports have been published concerning the improvement in the content of active components in *Epimedium* using an in vitro or in vivo method due to lack of mature biotechnologies, including in vitro regeneration (Ma et al. 2011a, b), in vitro hair root system, and transgenic system (Wang et al. 2012) in other species. Consequently, increasing the flavonoid content in *Epimedium* via induction by phytohormones has become an alternative.

In the present study, we isolated and characterized three *EsPALs*, given that the PAL enzyme channels the primary metabolite into phenylpropanoid enrichment in *Epimedium*. Gene expression and phytochemical assay were conducted to understand the roles of *EsPALs* in modulating different branch end-products biosynthesis in *Epimedium* phenylpropanoid pathway. Furthermore, the effects of phytohormones and sucrose on the expression of *EsPALs* and accumulation of flavonoids in *Epimedium* were evaluated.

Materials and methods

Epimedium samples and phytohormone treatment

All the diploid *Epimedium* plants tested were grown in the shadow in Wuhan Botanical Garden, China Academy of Sciences. *E. sagittatum* plants were used to isolate *PAL* genes. The inner sepals and petals of five *Epimedium* species, namely *E. acuminatum*, *E. mikinorii*, *E. leptorrhizum*, *E. franchetii*, and *E. sagittatum*, were chosen to establish the relationship between *EsPAL* expression and anthocyanin biosynthesis. The experimental results showed that the *E. sagittatum* H population contains a significantly higher level of active components than the L population. Subsequently, leaves in the H and L populations were harvested at different developmental stages to identify which *EsPAL* is in charge of the

biosynthesis of the active components in *Epimedium*. Samples that were designated as S1–S6 and used as temporal samples were cropped at completely curly leaves (S1), partially curly leaves (S2), completely expanding leaves (S3), one-fourth size of mature leaves (S4), one-half size of mature leaves (S5), and full size of mature leaves (S6). The content of lignin in leaves gained a steady increase from S1 to S6. The H2 and L6 lines, representing respectively the H and L populations, were selected for the characterization of the *EsPAL* expression and the phytochemical assay. In addition, roots, petioles, leaves, flowers, and siliques at the florescence stage were harvested and used as spatial samples. All samples were replicated three times and prepared for the assessment of the amount of *EsPAL* transcripts.

Epimedium pubescens plants were treated under light stress at 63 μE m^{-2} s^{-1} light intensity on day 1 and day 4 to investigate the effects of phytohormones and sucrose on the accumulation of flavonoids and to screen the optimum factors inducing flavonoids in *Epimedium* plants. Six-year-old *E. pubescens* plants with new growth roots were soaked in water mixed with 100 μM phytohormones [SA, abscisic acid (ABA), indole-3-acetic acid (IAA), or gibberellic acid (GA)] or 5 % sucrose, respectively. Subsequently, such treated plants were grown at 25 °C in a light bin (SPX-300B-G; Nanjing Ascent Technology Development Co., Ltd). At the same time, a control, designated as CK, was treated with pure water and grown in the same light bin. Triple specimens from each treatment were collected for the characterization of *EsPALs* in response to plant hormones or sucrose, and the ultimate quantitative assessment of transcript levels using real-time Polymerase Chain Reaction (RT-PCR).

Nucleotide extraction and isolation of *EsPALs*

DNA was extracted from young leaves of *E. sagittatum* as previously described (Porebski et al. 1997) and used as the template with which to amplify *EsPAL* genomic sequences. Total RNAs were extracted from *E. sagittatum* leaves using TRIzol Kit (Invitrogen, USA) according to the manufacturer's instructions and prepared for the amplification of *EsPAL* full-length CDS. An *Epimedium* 454-EST database (Zeng et al. 2010) was used for the isolation of full-length *EsPAL* ORF (Open Reading Frame) through the rapid amplification of cDNA ends (RACE) and the digital cloning. For EsPAL1, degenerate primers PAL-DF and PAL-DR were designed and a band of approximately 1,800 bp was amplified and sequenced. Based on the known sequence, the gene-specific primers 5-3EsPAL1 and 3-5EsPAL1 were designed and combined with SMARTIV and CDSIII primer for 5′RACE and 3′RACE, respectively. Finally, the gene-specific primers EsPAL1-FL-F and EsPAL1-FL-R were designed to confirm the full-length *EsPAL1* transcript. An approximate 2,200 bp fragment was obtained, resequenced, and checked. In addition, *EsPAL2* and *EsPAL3* were retrieved from the *Epimedium* 454-EST database. The EsPAL2-FL-F/EsPAL2-FL-R and EsPAL3-FL-F/EsPAL3-FL-R primer pairs were designed for confirming the full-length sequences of *EsPAL2* and *EsPAL3*, respectively. The detailed primer information of *EsPALs* was listed in Table 1. The *EsPAL* sequences were submitted to NCBI under accession numbers HQ331118, JQ319805, and JQ319806.

Sequence and phylogenetic tree analysis

PALs from the Phytozome database (http://www.phytozome.net/) were retrieved with default parameters for a comprehensive analysis of the *PAL* phylogeny in the Viridiplantae family. Detailed information for *PALs* is listed in Table S1. The genomic structure of *PAL* was predicted based on the Phytozome V7.0 database. For sequence analysis, ClustalX1.83 (Thompson et al. 1997) was used for sequence alignment with manual correction. A *PAL* phylogenetic tree was constructed via the Neighbor-Joining method using MEGA4.0 (Tamura et al. 2007). The isoelectric points and molecular weights of EsPALs were predicted by Compute pI/Mw (http://expasy.org/tools/pi_tool.html). Sequence identity and similarity between EsPALs were analyzed using EMBOSS Needle (http://www.ebi.ac.uk/Tools/psa/).

Gene expression analysis of *EsPALs*

To investigate the expression of *EsPAL* isoforms in another four *Epimedium* species, we isolated, sequenced, and confirmed the fragments representing each *EsPAL* isoform of the four *Epimedium* species. Total RNAs were isolated following the TRIzol protocol (Invitrogen, USA) for a quantitative test of the expression profile of EsPALs. The total RNAs were then reverse-transcribed using PrimeScript RT Reagent Kit with gDNA Eraser (DDR047; TaKaRa), which digested the residual DNA and reverse-transcribed RNA in one step. The *EsPAL* transcripts were amplified using SYBR Premix ExTaqTM^{II} (DDR081S; TaKaRa) and detected by an ABI 7500 Real-Time PCR system. The PCR program was set as follows: stage 1: 95 °C for 30 s, stage 2: 95 °C for 5 s followed by 60 °C for 34 s repeated for 40 cycles, and stage 3: 95 °C for 15 s, 60 °C for 1 min, and 95 °C for 15 s. Quantitative real-time PCR (qRT-PCR) experiments were performed in triplicate. The expression level of the *Epimedium* actin (*EsActin*) was used to standardize the RNA sample. The expression levels of *EsPALs* relative to *EsActin* were presented. In order to evaluate the levels of *EsPAL1*, *EsPAL2*, and *EsPAL3* transcripts, primer pairs were designed for qRT-PCR (Table 1).

Table 1 List of primers for *EsPALs* used in this study

Primer name	Sequence(5′–3′)	Note
PAL-DF	AARGGSACSGAYWSNTAYGGNGT	Core fragment
PAL-DR	GGSARNGGNGCNCCRTTCCA	
5-3EsPAL1	GCAATGTGTGAGAGGTTTCTGTTCCA	5′RACE
SMARTIV	AAGCAGTGGTATCAACGCAGAGTGGCCATTACGGCCGGG	
3-5EsPAL1	TTGCTCAACGGACAGAACGAGAAAGA	3′RACE
CDSIII	ATTCTAGAGGCCGAGGCGGCCGACATG-d$(T)_{30}$VN	
EsPAL1-FL-F	TTTTCTTTCTTTCTCCTTTCTCCC	Full length
EsPAL1-FL-R	AACCCTTACAACAAATGAACTTAC	
EsPAL2-FL-F	AGGATCTTCCTTTGGATCTACT	
EsPAL2-FL-R	TACGACTCTCTAACCACAATCA	
EsPAL3-FL-F	GTCCATCTTCACACCCAGTTGAGA	
EsPAL3-FL-R	AATAGACAACCACATGAGCCTCCA	
EsPAL1-RT-F	TAAAGAGGTAGAGAGCATGAGGAC	qRT-PCR
EsPAL1-RT-R	ATCAAAACAAAGAGAGTGAAAGAA	
EsPAL2-RT-F	GAGCGACAATGCGGCTATCCCTAA	
EsPAL2-RT-R	TCACCAGTCAACAATGCAGTTCCC	
EsPAL3-RT-F	GCCAGAAAGACACTGAGTATCGGA	
EsPAL3-RT-R	ATGGGTCGTCAATGTAGGTGAAAA	
EsActin-RT-F	TACGAACAGGAGCTGGAGACTT	
EsActin-RT-R	GATGGTCCAGACTCGTCATACTC	

Phytochemical determination

For the analysis of active components, approximately 50 mg of ground sample was soaked in 5 ml of 70 % ethanol and ultrasonicated for 30 min before being filtrated through 0.45 μm polyfilters for HPLC analysis. HPLC under 272 nm wavelength was carried out at a flow rate of 1.0 ml/min on Agilent Technologies Series 1100 (Agilent Technologies, Palo Alto, CA, USA). Zorbax SB-C18 chromatographic columns (250 mm × 4.6 mm I.D., 5 μm; Agilent Technologies) were used at 25 °C. The mobile phase consisted of acetonitrile and 36 % acetic acid. Data analysis was performed using Agilent ChemStation (VA.10.02). Epimedin A, epimedin B, epimedin C, and icariin standards were purchased from ChromaDex (Santa Ana, USA).

For the anthocyanin assay, separated sepals and petals of five different *Epimedium* species were harvested and powdered using liquid nitrogen for anthocyanin extraction using a previously described method with modifications (Mancinelli 1984). Approximately 0.2 g of powders was soaked in 10 ml of acidic methanol (0.1 % HCl, v/v) buffer at 4 °C for 24 h. Subsequently, the mixture was centrifuged at 3,000 rpm for 10 min, and the supernatant was collected to measure the A530 and A657 values using a U-3900 spectrophotometer (Hitachi High-Tech, Japan). Finally, the relative content of anthocyanin in each specimen was calculated as follows: (A530 − 0.25 * A657)/Fresh Weight (g). The data reported for sepals and petals of the *Epimedium* species represented the mean values of three replicates. For the total flavonoid assessment, leaf samples from phytohormone- and sucrose-treated *E. pubescens* plants were harvested and dried by silica gel before they were ground using liquid nitrogen. A sample of approximately 20 mg was used to extract the total flavonoid following a previously reported method with minor modifications (Zhang et al. 2008). The ground sample was soaked in 30 ml of ethanol (50 %) and ultrasonicated at 50 °C for 90 min. Subsequently, the filtrate was collected through a 0.22 μm microporous membrane. Finally, the total flavonoid content was quantified using a U-3900 spectrophotometer at 270 nm.

Results

Isolation and sequence analysis of *EsPALs*

We isolated *EsPAL1*, *EsPAL2*, and *EsPAL3* mRNA sequence, encoding respectively 709, 716, and 739 amino acids, with the theoretical isoelectric point/molecular weight values being 6.07/77,353.6 Da for EsPAL1, 5.83/77,705.7 Da for EsPAL2, and 6.23/80,315.3 Da for EsPAL3. The protein identities/similarities of EsPAL1/EsPAL2, EsPAL1/EsPAL3, and EsPAL2/EsPAL3 were calculated as 84.9/92.9 %, 60.8/74.1 %, and 62.0/73.8 %, respectively, suggesting that *EsPAL1* is closer to *EsPAL2* than to *EsPAL3*,

which was confirmed by sequence alignment (Fig. S1), genomic structure (Fig. 2a), and phylogenetic tree (Fig. 2b). As shown in Fig. S1, the predicted active residues, MIO group (Ala–Ser–Gly triad), and phosphorylation residues are conserved in EsPALs and ArthPAL1 (Allwood et al. 1999). The predicted substrate specificities of F127 in EsPAL1, F135 in EsPAL2, and F157 in EsPAL3 are also highly conserved to F134 in BaolPAL2/3 that has PAL activity (Hsieh et al. 2010), suggesting that EsPALs possess PAL activity.

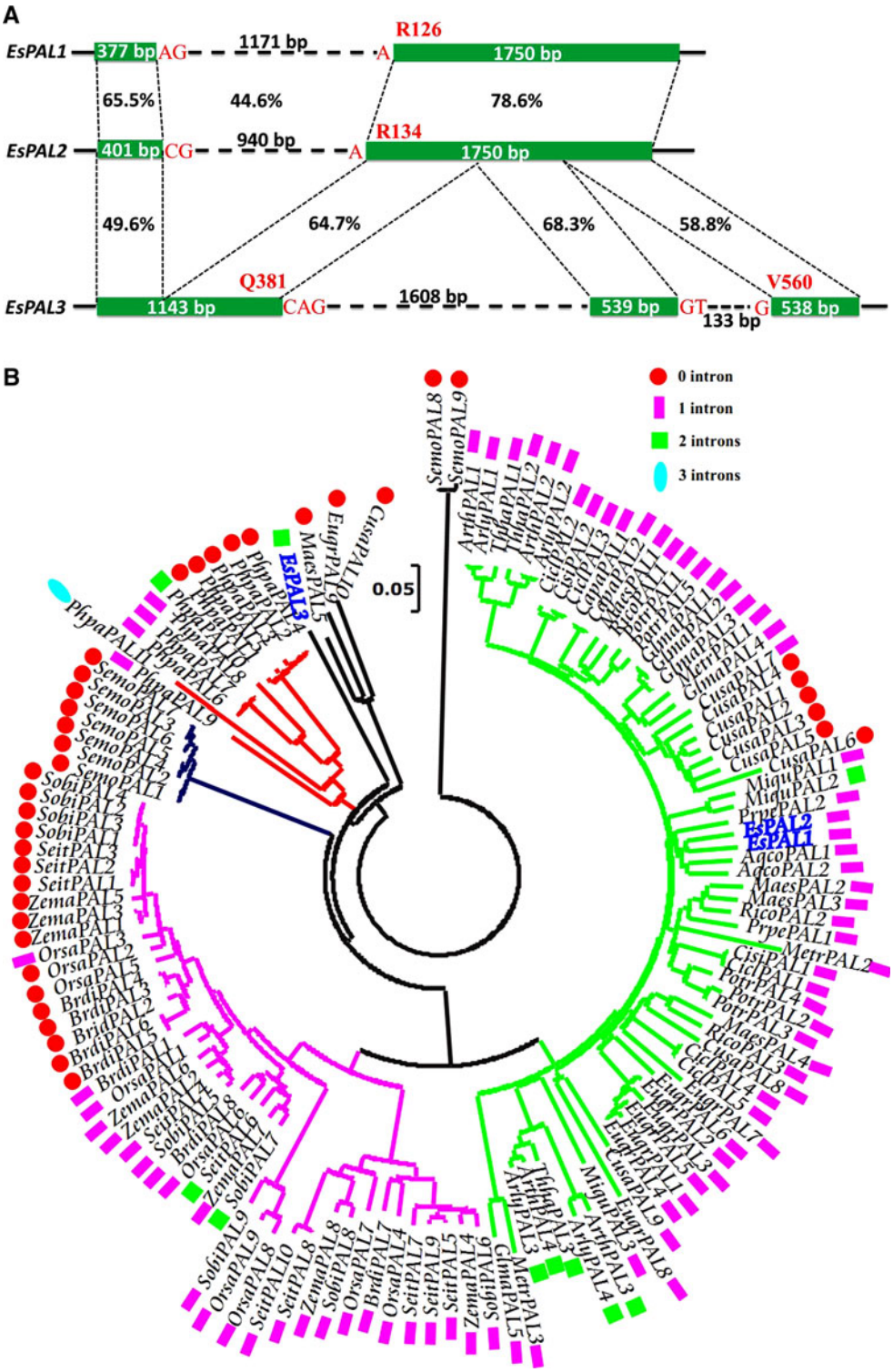

Fig. 2 Genomic structure (**a**) and Neighbor-Joining phylogenetic tree (**b**) of *EsPALs*. The numbers labeled in the exon *box* or on the intron *line* represents the sizes of the exon and intron, respectively. The codons in *red*, interrupted by an intron, correspond to amino acids on top of the exons. Percentages indicate the similarity of fragments between EsPALs. Detailed information of the model species *PALs* is listed in Table S1. Sequence alignment was performed by ClustalX1.83 and corrected manually. An NJ tree was constructed using MEGA4.0 with 1000 bootstrap replicates. *Light green*, *light purple*, *blue*, and *red* branches represent the dicot PAL, monocot PAL, SemoPAL, and PhpaPAL subgroups, respectively. Furthermore, the *closed red circle*, *light purple rectangle*, *light green square*, and *light blue oval* near the PALs in the phylogenetic tree represent the numbers of introns present: zero, one, two, and three, respectively. (Color figure online)

Tissue expression profiles of *EsPALs*

To dissect the spatiotemporal expression profiles of *EsPALs*, roots, petioles, leaves, flowers, and siliques of *E. sagittatum* were harvested at florescence stage S4 for qRT-PCR. As shown in Fig. 3, the expression patterns of *EsPAL1* and *EsPAL2* were conserved and abundant in roots. *EsPAL3* transcripts were remarkably enriched in leaves, flowers, and siliques, where flavonoid, anthocyanin, and proanthocyanin are generally considered to be enriched.

Profiles of *EsPAL* expression and active components in leaves of *E. sagittatum*

In order to identify the *EsPAL* isoform modulating the biosynthesis of active compounds in *Epimedium*, we investigated the profile of *EsPALs* expression and accumulation of active components in S1–S6 leaf samples in H2 and L6 line, which represent *Epimedium* populations with a high and low level of active components, respectively. As presented in Fig. 4a, c, the *EsPAL3* expression pattern is in perfect agreement with the accumulation trend of active components in the H2 line, except that the content of the active components peaks at S5 while the *EsPAL3* transcript peaks at S4. In contrast, *EsPAL1* and *EsPAL2* were highly expressed in S4–S6 (Fig. 4a), during which *Epimedium* leaves begin to mature and turn leathery, along with increased lignification as observed in line L6 (Fig. 4b, d). As shown in Fig. 4, the metabolite accumulation lags behind the gene expression of *EsPALs*. The high level of *EsPAL2* transcript accounts partially, if not completely, for the peak of active components at S5 in the H2 and L6 lines (Fig. 4). In addition, the comparative analysis reveals that the *EsPAL3* transcript level is lower in the L6 line than in the H2 line at S3 and S4, which might account for the lower content of active components in the L6 line than in the H2 line (Fig. 4).

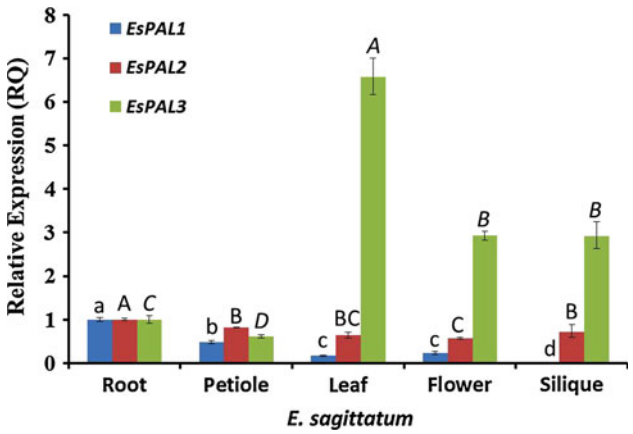

Fig. 3 Spatial expression pattern of *EsPALs* in *E. sagittatum*. *Vertical bars* indicate the standard deviation of three replicates. Mean ± SD determined from three independent samples are shown. *Different letters* indicate significant differences in gene expression of each *EsPAL* isoform in different tissues as calculated by Duncan statistical analysis ($P < 0.01$)

EsPAL3 is predominantly involved in anthocyanin biosynthesis in *Epimedium*

To determine which *EsPAL* isoforms being responsible for the anthocyanin biosynthesis, we investigated the *EsPAL* expression patterns in the sepals and petals of five *Epimedium* species with different colors (Fig. 5a). Under our detection system, *EsPAL1* transcripts were not detected in the petals and sepals of all five *Epimedium* species (data not shown). The *EsPAL3* expression profile was perfectly coincident with the color phenotypes in *E. acuminatum* and *E. leptorrhizum* (Fig. 5a, c), where tissue(s) with a high level of anthocynain express a high level of *EsPAL3* transcripts (Fig. 5b, c). However, the number of *EsPAL2* transcripts was smaller than that of *EsPAL3* transcripts (Fig. 5c). Low anthocyanin levels were detected in *E. franchetii* and *E. sagittatum* (Fig. 5b), although *EsPAL3* was highly expressed in petals of both species (Fig. 5c), suggesting that anthocyanin biosynthesis in the two species was blocked in the downstream of the PAL committed step. Surprisingly, both *EsPAL2* and *EsPAL3* exhibited a slightly higher expression in the white inner sepal than in the orchid petal of *E. mikinorii* (Fig. 5c), and they accumulated at a lower level than their counterparts in *E. acuminatum* and *E. leptorrhizum* petals (Fig. 5c), suggesting that another *Epimedium PAL* member may control the anthocyanin biosynthesis in *E. mikinorii*. Alternatively, there may exist certain trans-regulators, such as transcription factors like MYB and bHLH, which may negatively regulate anthocyanin genes in sepals, resulting in less anthocyanin accumulation in sepals than in petals. For instance, *FaMYB1* (Aharoni et al. 2001) and *MdMYB6* (Gao et al. 2011) have been reported to repress the anthocyanin in transgenic plants.

Effects of phytohormones and sucrose on *EsPAL* expression

As a result of lack of mature biotechnologies, including in vitro regeneration, in vitro hair root system, and transgenic system, phytohormones and sucrose induction has become an alternative to improve the content of active components in *Epimedium*. In the SA sample, *EsPAL1* transcripts were downregulated, but *EsPAL2* and *EsPAL3* were enhanced on the fourth day as compared with the CK sample (Fig. 6a–c). For the GA_3 sample, *EsPAL1* and *EsPAL2* were remarkably induced by GA_3 on the first day and decreased thereafter, whereas *EsPAL3* was

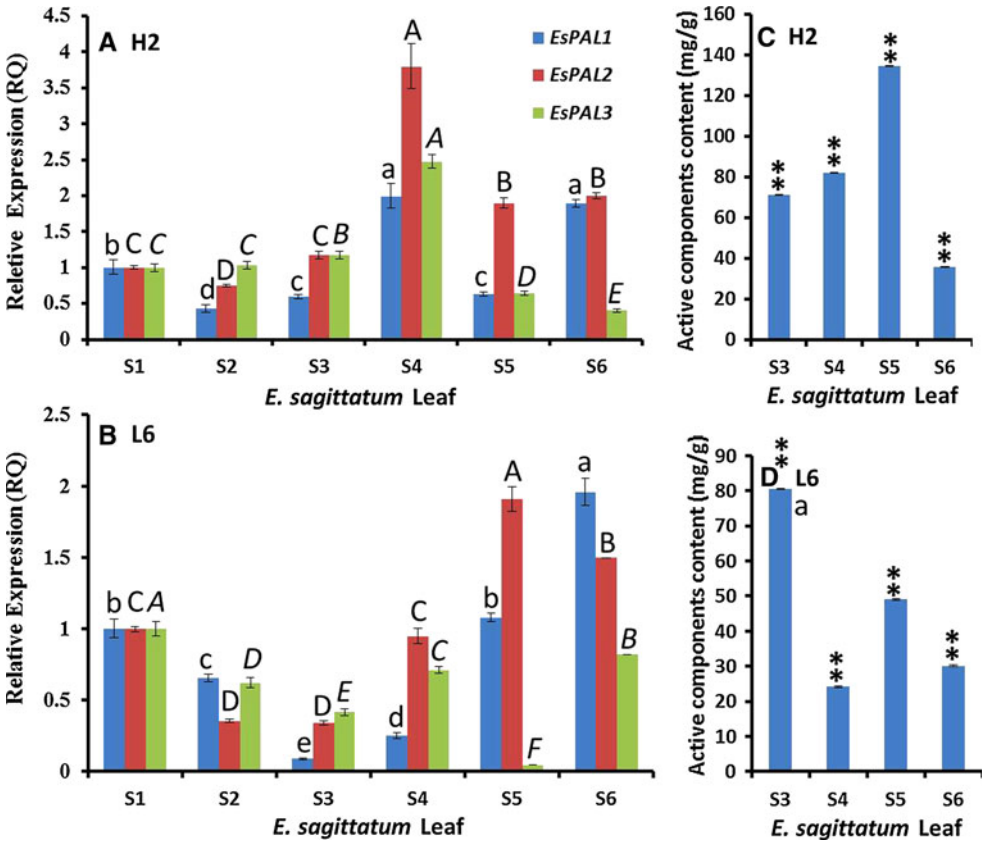

Fig. 4 Differential expression profiles of *EsPALs* (**a**, **b**) and the accumulation patterns of active components (**c**, **d**) in leaves of *E. sagittatum* from H and L populations at five developmental stages. Active components represent icariin, epimedin A, epimedin B, and epimedin C. Mean ± SD determined from three independent samples are shown. *Different letters* and *double stars* respectively indicate significant differences in gene expression of each *EsPAL* isoform in different stages (**a**, **b**) and the content of active components (**c**, **d**) in leaves at different developmental stages as calculated by Duncan statistical analysis ($P < 0.01$)

continuously increased (Fig. 6a–c). For the ABA treatment, *EsPAL2* and *EsPAL3* transcript levels were reduced on the first day and increased to the level of CK sample. On the contrary, *EsPAL1* was constant on the first day and upregulated on the fourth day as compared with the CK sample (Fig. 6a–c). For IAA, there was no statistic difference of *EsPALs* transcript level compared to CK sample, except that *EsPAL2* transcripts increased on the first day and *EsPAL1* was downregulated on the fourth day (Fig. 6a–c). In the sucrose sample, a continuous increase was detected in the transcript levels of *EsPAL2* and *EsPAL3* in response to sucrose (Fig. 6a, b). In contrast, *EsPAL1* transcripts increased significantly initially and then sharply decreased (Fig. 6c).

Effects of phytohormones and sucrose on flavonoid accumulation in *Epimedium*

Assessing the trend of flavonoids in response to phytohormones and sucrose is a prerequisite in drafting strategies for improving the content of active components in *Epimedium* to increase production for human consumption while minimizing the damage to wild resources of *Epimedium* caused by commercial overexploitation. As shown in Fig. 6d, the total flavonoid content in the CK sample decreased under light stress. In the SA and GA_3 samples, the flavonoid content was continuously enhanced when compared with the CK sample. On contrary, the total flavonoid level increased on the first day and decreased on the fourth day in IAA, Sucrose, and ABA samples, although the total flavonoid content was enhanced compared with that in the CK sample (Fig. 6d).

Discussion

Phenylalanine ammonia-lyase concatenates primary and secondary metabolites by carrying out the first catalysis step in the biosynthesis of the phenylpropanoid pathway. The active components in *Epimedium* are a major subset of flavonoid products derived from phenylpropanoid pathway. Although many PAL genes, consisting of small gene family, were isolated and characterized in many species, the characteristics of *Epimedium* PAL are still unclear. In this study, three *PAL* genes were isolated. *EsPAL1*, *EsPAL2*, and *EsPAL3* encode 709, 716, and 739 amino acids, respectively. Our results show that *EsPAL1* is closer to *EsPAL2* than to *EsPAL3*, which has been confirmed by sequence alignment (Fig. S1), genomic structure (Fig. 2a), and phylogenetic tree (Fig. 2b).

Based on the results shown in Figs. 3, 4, and 5, we can draw two tentative conclusions: (1) *EsPAL3* and, to a lesser

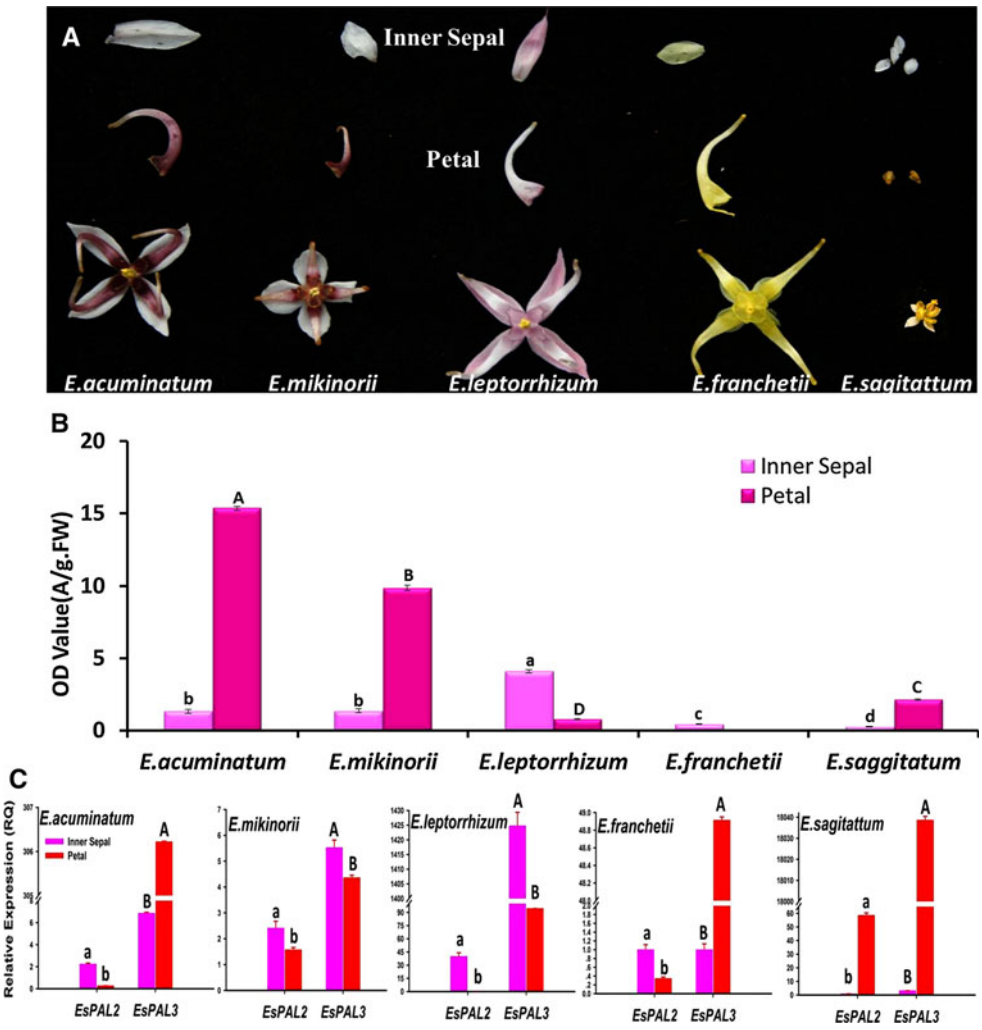

Fig. 5 The color phenotype (**A**) anthocyanin content (**B**) and *EsPAL* expression patterns (**C**) in separated sepals and petals of five *Epimedium* species. Mean ± SD determined from three independent samples are shown. *Different letters* indicate significant differences in the anthocyanin content in the petal or sepal of five different species (**B**) and the gene expression of *EsPAL2* or *EsPAL3* isoform in petal and sepal of certain species (**C**) as calculated by Duncan statistical analysis ($P < 0.01$)

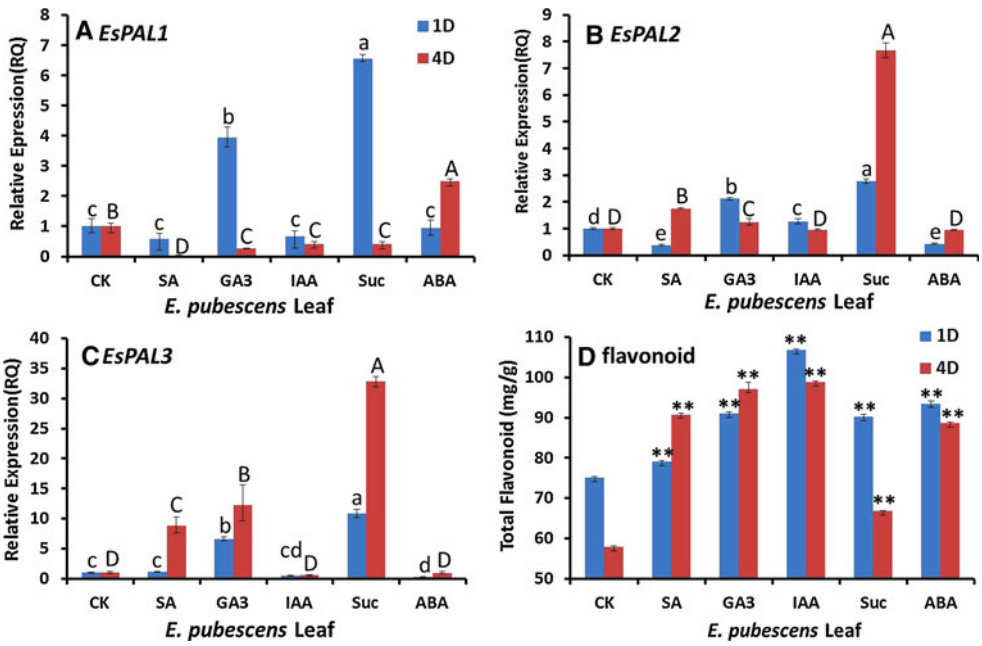

Fig. 6 Effects of phytohormones and sucrose on the expressions of *EsPAL1* (**a**), *EsPAL2* (**b**) and *EsPAL3* (**c**), and the accumulation pattern of total flavonoid (**d**) in *E. pubescens*. Mean ± SD determined from three independent samples are presented. *Different letters* and *double stars* respectively indicate significant differences in the gene expression of each EsPAL isoform in different treatments (**a**–**c**) and the flavonoid content (**d**) in samples treated on day one and day four as calculated by Duncan statistical analysis ($P < 0.01$)

extent, *EsPAL2* are in charge of funneling metabolic flux into flavonoid secondary metabolism toward flower pigments (anthocyanin), UV-protective flavonol derivatives and proanthocyanins; (2) *EsPAL1* and *EsPAL2* are involved in the lignin biosynthesis. The two conclusions are supported by the following observations: (a) *EsPAL3* transcripts are abundant in flavonoid-enriched tissues, including leaves, flowers, and siliques, in which *EsPAL2* and *EsPAL1* transcripts are low or undetectable (Fig. 3). (b) The expression pattern of *EsPAL3*, but not *EsPAL1*, perfectly matches the accumulation profile of active components in different developmental stages of leaves (Fig. 4). *EsPAL2* contributes at a lesser extent to flavonoid biosynthesis at S4–S6 (Fig. 4). (c) The expression patterns of *EsPAL1* and *EsPAL2* are in accordance with the extent of increasingly elevated lignification in mature leaves from S4 to S6 (Fig. 4a, b). (d) *EsPAL3* and *EsPAL2* account for the anthocyanin biosynthesis in the sepals and petals of *Epimedium* (Fig. 5). *EsPAL3* transcripts highly accumulated in the sepals and petals of the five *Epimedium* species with different colors, whereas *EsPAL2* was expressed at a low level and *EsPAL1* transcripts were undetectable (Fig. 5). Altogether, *EsPALs* have experienced functional diversity in their evolutionary history, resulting in the branch-preference expressions of *EsPAL1* for the lignin pathway, *EsPAL3* for the flavonoid and anthocyanin pathways, and *EsPAL2* for the lignin, flavonoid, and anthocyanin pathways (Figs. 2, 3, 4). We previously found that *Es4CL1* and *Es4CL2* channel the metabolic flux into the lignin and flavonoid pathways in *Epimedium*, respectively (Huang et al., unpublished data). It could be concluded that *EsPAL1/2* paralleling with *Es4CL1* and *EsPAL2/3* paralleling with *Es4CL2* are responsible for lignin and flavonoid biosynthesis, respectively. In *P. tremuloides*, the gene expressions of *PtPAL1* and *PtPAL2*, paralleling with *Pt4CL2* and *Pt4CL1*, respectively, are associated with proanthocyanidin and lignin biosynthesis (Kao et al. 2002). Similarly, Arabidopsis *4CL3* and *4CL1/2*, which differ in their substrate preferences and expression patterns, have been reported to be responsible for the biosynthesis of flavonoids and lignins and other phenolics, respectively (Ehlting et al. 1999; Humphreys and Chapple 2002). In summary, the differential expressions among the gene family members involved in the phenylpropanoid pathway encode distinct enzyme isoforms, distinguish substrate selectivity, and form distinct membrane-associated metabolons, which further dedicate to different end-products of phenylpropanoid branches (Winkel 2004). *Epimedium* likely adopts these strategies to function divergently in both *EsPALs* and *Es4CLs* and produce various phenylpropanoid end-products.

In this study, the effects of phytohormone and sucrose on *EsPALs* expression and flavonoid accumulation in *Epimedium* were also investigated. As presented in Fig. 6b–d, the expression patterns of *EsPAL2* and *EsPAL3* were in accordance with the flavonoid profile in the SA sample and thus *EsPAL2* and *EsPAL3*, especially *EsPAL3*, might account for the increase of the flavonoid content in the SA sample. One recent study has documented that the phenylpropanoid pathway may be responsible for the production of a regulatory molecule for SA biosynthesis or accumulation (Huang et al. 2010). Consequently, it can be deduced that exogenous SA and light stress-induced endogenous SA may regulate phenylpropanoid biosynthesis in a feedback manner. When applied, the exogenous SA initially blocks SA biosynthesis and then further channels the metabolic flux into the flavonoid pathway, playing a larger role over the effect of SA-induced depression of *EsPALs*, until a tradeoff is achieved, which determines the flavonoid content on the first day (Fig. 6d). In contrast, the enhanced *EsPAL2* and *EsPAL3* transcripts contributed to the high flavonoid content on the fourth day (Fig. 6b, c). For the GA_3 sample, the sharp enhancement of *EsPAL* transcripts resulted in a high flavonoid content (Fig. 6d). *EsPALs* expression patterns suggested that *EsPAL1* and *EsPAL3* might be responsible for the high content of flavonoids on the first day, whereas *EsPAL3* might dominate the flavonoid accumulation on the fourth day (Fig. 6). The transcripts of genes, including *PAP1*, *F3'H*, *LDOX*, and *UF3GT*, were highly accumulated in Arabidopsis under low phosphate conditions, and GA treatment rapidly reduced the amount of these transcripts (Jiang et al. 2007). In the present study, GA_3 treatment possibly blocked anthocyanin biosynthesis in *E. pubescens* cultured with water, resulting in the accumulation of an anthocyanin precursor, dihydroflavonol (Fig. 6d). In addition, GA_3 application increased CHS and CHI mRNA levels, as well as the protein level in *Petunia hybrida* (Weiss et al. 1990). Taken together, the integrative signals of hormone (GA) and abiotic stress (light stress and phosphate deficiency) promote the expression of upstream genes in the flavonoid pathway and decrease the expression of downstream genes in the anthocyanin pathway, which might account for the accumulation of higher levels of flavonoids in the GA_3 sample (Fig. 6d). Previous studies demonstrated that ABA lessens the activity of PAL at molecular and biochemical levels (Ward et al. 1989). At the same time, a previous study reported that ABA enhances the mRNA level and enzymatic activity of PAL in grape (Jeong et al. 2004). Furthermore, ABA treatment promotes anthocyanin and phenolic accumulation in strawberry (Jiang and Joyce 2003). In *Epimedium*, the flavonoid content in the ABA sample was higher than that in the CK sample and approached the level in the RT sample, suggesting that the effect of ABA-enhanced EsPAL enzymatic activity might overwhelm the effect of ABA-suppressed *EsPAL* expression (Fig. 6). For IAA, *EsPAL2* transcripts enhanced significantly on the first day, which might account

for the increase of the flavonoid content in the IAA sample (Fig. 6). Recently, IAA-induced signals were found to upregulate flavonoid-related genes, including *AtCHS*, *AtCHI*, *AtFLS*, and *AtMYB12* (Lewis et al. 2011). Perhaps, IAA signals could also activate the flavonoid structural genes and promote the flavonoid biosynthesis in *Epimedium*, although only *EsPAL2* transcripts were enhanced on the first day (Fig. 6a–c). In the sucrose sample, the expression pattern of *EsPAL1* was perfect in accordance with the accumulation pattern of flavonoid, suggesting that *EsPAL1* might play a larger role than *EsPAL2* and *EsPAL3* in the flavonoid biosynthesis under sucrose treatment (Fig. 6).

In conclusion, three *EsPALs* were isolated and characterized in the present study. Sequence analysis indicated that EsPALs possess PAL activity as in model species. Sequence alignment, phylogeny, and genome structure showed that *EsPAL1* shares a higher level of identity with *EsPAL2* than with *EsPAL3*. Gene expression profiles and flavonoid accumulation patterns revealed that *EsPAL1* and *EsPAL2* may be in charge of lignin biosynthesis, whereas *EsPAL3* and, to a lesser extent, *EsPAL2* may account for flavonoid and anthocyanin biosynthesis. Our findings suggest that *EsPALs* play a pivotal role in modulating the metabolic flux into different branches of the phenylpropanoid pathway, resulting in abundant phenolic compounds in *Epimedium.* Furthermore, under light stress, SA, GA, IAA, ABA, and sucrose can promote flavonoid accumulation in *Epimedium* via activating different *EsPAL* isoform(s).

Acknowledgments This work was supported by the South China Botanical Garden Startup Fund (201039), the CAS/SAFEA International Partnership Program for Creative Research Teams Project, the Knowledge Innovation Project of the Chinese Academy of Sciences (KSCX2-EW-J-20), and the National Natural Science Foundation of China (30800624). We thank Qiaoyan Xiang for helping with the anthocyanin analysis and Di Liu for proofreading this manuscript.

References

Aharoni A, De Vos CHR, Wein M, Sun Z, Greco R, Kroon A, Mol JNM, O'Connell AP (2001) The strawberry *FaMYB1* transcription factor suppresses anthocyanin and flavonol accumulation in transgenic tobacco. Plant J 28(3):319–332. doi:10.1046/j.1365-313X.2001.01154.x

Allwood EG, Davies DR, Gerrish C, Ellis BE, Bolwell GP (1999) Phosphorylation of phenylalanine ammonia-lyase: evidence for a novel protein kinase and identification of the phosphorylated residue. FEBS Lett 457:47–52. doi:10.1016/S0014-5793(99)00998-9

Committee CP (2005) Herba epimedii. In: Committee CP (ed) Pharmacopoeia of the People's Republic of China. Chemical Industry Press, Beijing, p 229

Ehlting J, Büttner D, Wang Q, Douglas CJ, Somssich IE, Kombrink E (1999) Three 4-coumarate: coenzyme A ligases in *Arabidopsis thaliana* represent two evolutionarily divergent classes in angiosperms. Plant J 19:9–20. doi:10.1046/j.1365-313X.1999.00491.x

Gao J, Shen X, Zhang Z, Peng R, Xiong A, Xu J, Zhu B, Zheng J, Yao Q (2011) The myb transcription factor *MdMYB6* suppresses anthocyanin biosynthesis in transgenic *Arabidopsis*. Plant Cell Tissue Organ Cult 106:235–242. doi:10.1007/s11240-010-9912-4

Guo J, Wang MH (2009) Characterization of the phenylalanine ammonia-lyase gene (*SlPAL5*) from tomato (*Solanum lycopersicum* L.). Mol Biol Rep 36:1579–1585. doi:10.1007/s11033-008-9354-9

Hsieh L, Ma G, Yang C, Lee P (2010) Cloning, expression, site-directed mutagenesis and immunolocalization of phenylalanine ammonia-lyase in *Bambusa oldhamii*. Phytochemistry 71:1999–2009. doi:10.1016/j.phytochem.2010.09.019

Huang J, Gu M, Lai Z, Fan B, Shi K, Zhou Y, Yu J, Chen Z (2010) Functional analysis of the Arabidopsis PAL gene family in plant growth, development, and response to environmental stress. Plant Physiol 153:1526–1538. doi:10.1104/pp.110.157370

Humphreys JM, Chapple C (2002) Rewriting the lignin roadmap. Curr Opin Plant Biol 5:224–229. doi:10.1016/s1369-5266(02)00257-1

Jeong ST, Goto-Yamamoto N, Kobayashi S, Esaka A (2004) Effects of plant hormones and shading on the accumulation of anthocyanins and the expression of anthocyanin biosynthetic genes in grape berry skins. Plant Sci 167:247–252. doi:10.1016/j.plantsci.2004.03.021

Jiang YM, Joyce DC (2003) ABA effects on ethylene production, PAL activity, anthocyanin and phenolic contents of strawberry fruit. Plant Growth Regul 39:171–174. doi:10.1023/A:1022539901044

Jiang C, Gao X, Liao L, Harberd NP, Fu X (2007) Phosphate starvation root architecture and anthocyanin accumulation responses are modulated by the gibberellin-DELLA signaling pathway in Arabidopsis. Plant Physiol 145:1460–1470. doi:10.1104/pp.107.103788

Kao Y, Harding SA, Tsai C (2002) Differential expression of two distinct phenylalanine ammonia-lyase genes in condensed tannin-accumulating and lignifying cells of quaking aspen. Plant Physiol 130:796–807. doi:10.1104/pp.006262

Lewis DR, Ramirez MV, Miller ND, Vallabhaneni P, Ray WK, Helm RF, Winkel BSJ, Muday GK (2011) Auxin and ethylene induce flavonol accumulation through distinct transcriptional networks. Plant Physiol 156:144–164. doi:10.1104/pp.111.172502

Ma G, da Silva JAT, Lue J, Zhang X, Zhao J (2011a) Shoot organogenesis and plant regeneration in *Metabriggsia ovalifolia*. Plant Cell Tissue Organ Cult 105:355–361. doi:10.1007/s11240-010-9875-5

Ma G, Lue J, da Silva JAT, Zhang X, Zhao J (2011b) Shoot organogenesis and somatic embryogenesis from leaf and shoot explants of *Ochna integerrima* (Lour). Plant Cell Tissue Organ Cult 104:157–162. doi:10.1007/s11240-010-9812-7

Ma H, He X, Yang Y, Li M, Hao D, Jia Z (2011c) The genus *Epimedium*: an ethnopharmacological and phytochemical review. J Ethnopharmacol 134:519–541. doi:10.1016/j.jep.2011.01.001

Mancinelli AL (1984) Photoregulation of anthocyanin synthesis: VIII. Effect of light pretreatments. Plant Physiol 75:447–453. doi:10.1104/pp.75.2.447

Park JH, Park NI, Xu H, Park SU (2010) Cloning and characterization of phenylalanine ammonia-lyase and cinnamate 4-hydroxylase and pyranocoumarin biosynthesis in *Angelica gigas*. J Nat Prod 73:1394–1397. doi:10.1021/np1003356

Porebski S, Bailey LG, Baum BR (1997) Modification of a CTAB DNA extraction protocol for plants containing high polysaccharide and polyphenol components. Plant Mol Biol Rep 15:8–15. doi:10.1007/BF02772108

Reichert AI, He XZ, Dixon RA (2009) Phenylalanine ammonia-lyase (PAL) from tobacco (*Nicotiana tabacum*): characterization of the four tobacco PAL genes and active heterotetrameric enzymes. Biochem J 424:233–242. doi:10.1042/bj20090620

Song J, Wang Z (2009) Molecular cloning, expression and characterization of a phenylalanine ammonia-lyase gene (*SmPAL1*) from *Salvia miltiorrhiza*. Mol Biol Rep 36:939–952. doi:10.1007/s11033-008-9266-8

Tamura K, Dudley J, Nei M, Kumar S (2007) MEGA4: molecular evolutionary genetics analysis (MEGA) software version 4.0. Mol Biol Evol 24:1596–1599. doi:10.1093/molbev/msm092

Thompson JD, Gibson TJ, Plewniak F, Jeanmougin F, Higgins DG (1997) The CLUSTAL_X windows interface: flexible strategies for multiple sequence alignment aided by quality analysis tools. Nucleic Acids Res 25:4876–4882. doi:10.1093/nar/25.24.4876

Tong JS, Zhang QH, Huang X, Fu XQ, Qi ST, Wang YP, Hou Y, Sheng J, Sun QY (2011) Icaritin causes sustained ERK1/2 activation and induces apoptosis in human endometrial cancer cells. PLoS ONE 6:e16781. doi:10.1371/journal.pone.0016781

Wang C, Hsu S, Chen P, To K (2012) Transformation and characterization of transgenic *Bidens pilosa* L. Plant Cell Tissue Organ Cult 109:457–464. doi:10.1007/s11240-011-0110-9

Ward EWB, Cahill DM, Bhattacharyya MK (1989) Abscisic acid suppression of phenylalanine ammonia-lyase activity and mRNA, and resistance of soybeans to *Phytophthora megasperma* f.sp. glycinea. Plant Physiol 91:23–27. doi:10.1104/pp.91.1.23

Weiss D, Vantunen AJ, Halevy AH, Mol JNM, Gerats AGM (1990) Stamens and gibberellic acid in the regulation of flavonoid gene expression in the corolla of *Petunia hybrida*. Plant Physiol 94:511–515. doi:10.1104/pp.94.2.511

Winkel BSJ (2004) Metabolic channeling in plants. Annu Rev Plant Biol 55:85–107. doi:10.1146/annurev.arplant.55.031903.141714

Xu F, Cai R, Cheng SY, Du HW, Wang Y, Cheng SH (2008) Molecular cloning, characterization and expression of phenylalanine ammonia-lyase gene from *Ginkgo biloba*. Afr J Biotechnol 7:721–729

Zeng SH, Xiao G, Guo J, Fei ZJ, Xu YQ, Roe BA, Wang Y (2010) Development of a EST dataset and characterization of EST-SSRs in a traditional Chinese medicinal plant, *Epimedium sagittatum* (Sieb. Et Zucc.) Maxim. BMC Genomics 11:94. doi:10.1186/1471-2164-11-94

Zhang HF, Yang TS, Li ZZ, Wang Y (2008) Simultaneous extraction of epimedin A, B, C and icariin from *Herba Epimedii* by ultrasonic technique. Ultrason Sonochem 15:376–385. doi:10.1016/j.ultsonch.2007.09.002

Zhu JF, Li ZJ, Zhang GS, Meng K, Kuang WY, Li J, Zhou XF, Li RJ, Peng HL, Dai CW, Shen JK, Gong FJ, Xu YX, Liu SF (2011) Icaritin shows potent anti-leukemia activity on chronic myeloid leukemia in vitro and in vivo by regulating MAPK/ERK/JNK and JAK2/STAT3/AKT signalings. PLoS ONE 6:e23720. doi:10.1371/journal.pone.0023720